9th Asia-Pacific Conference on Wind Engineering
Auckland, New Zealand
3-7 December 2017

Aerodynamic stabilization and robustness evaluation of cable-supported bridges

Y.J. Ge

State Key Laboratory of Disaster Reduction in Civil Engineering
Tongji University, Shanghai 200092, China

Abstract

Cable-supported bridges with cable-stayed and suspension types, are becoming longer, lighter and less damped, and accordingly are facing sever aerodynamic problems, in particular, aerodynamic flutter and aerostatic divergence. The dynamic and aerodynamic performance of top five long-span cable-stayed bridges have been compared, and followed by the introduction of cantilever horizontal stabilization plate and twin box deck for aerodynamic stabilization of longer spans of 1400~1500m. After the technical review of three types of effective stabilization countermeasures for suspension bridges, including stabilizer, slot and their combination, the challenging stabilization for longer suspension bridges has been introduced with some new attempts, for example, horizontal stabilizers, combination of vertical and horizontal stabilizers, optimization of twin box girder and widely slotted box girder or narrowly slotted box girder with stabilizers. Based on probabilistic model and the first order second moment approach, the robustness evaluation method has been proposed to estimate aerodynamic instability of long-span cable-supported bridges with the main index of return period.

Introduction

Cable-supported bridges are basically composed of three main elements including cable, pylon and deck, and can be divided into two main types, cable-stayed bridge and suspension bridge with greater bridging capacity. The evolution of span length of these two types of cable-supported bridges greatly promotes the development of modern bridge engineering and advanced bridge aerodynamics [1].

No	Year	Bridge Name	Span(m)	Girder
1	1883	Brooklyn	486	Truss
2	1903	Williamsburg	488	Truss
3	1924	Bear Mountain	497	Truss
4	1926	Benjamin Franklin	533	Truss
5	1929	Ambassador	564	Truss
6	1931	George Washington	1,067	Truss
7	1937	Golden Gate	1,280	Truss
8	1964	Verrazano Narrows	1,298	Truss
9	1981	Humber	1,410	Box
10	1998	Storebaelt East	1,624	Box
11	1998	Akashi Kaikyo	1,991	Truss
12	2009	Xihoumen	1,650	Box

Table 1. Record-breaking suspension bridges.

Modern suspension bridges are come from rattan chain and later iron chain supported bridges, which were invented and created in China in ancient time, and have experienced a considerable development since 1883, when the first modern suspension bridge, Brooklyn Bridge, was built with a span length of 486m. It took about 48 years for the span length of suspension bridges to jump to 1,067m of George Washington Bridge in 1931, as the first bridge with a span length over 1,000m. Although the further increase in the next 50 years was not so large in Humber Bridge of 1,410m in 1981, the new stiffening girder, orthotropic steel box girder, replaced the traditional steel truss girder. The latest span length record has been hold by 1,991m Akashi Kaikyo Bridge with truss girder built in 1998 and 1,650m Xihoumen Bridge with box girder in 2009. Table 1 shows twelve suspension bridges with a record-breaking span length in the history after Brooklyn Bridge [2].

Although cable-stayed bridges can be traced back to the 18th century, Strömsund Bridge completed in 1955 is often cited as the first modern cable-stayed bridge with a main span of 183m. It took about 20 years for the span length of cable-stayed bridges to enlarge to 404m in Saint-Nazaire Bridge in 1975 with an increase factor of 2.2, and the same increase factor was achieved within next 24 years in the 890m Tatara Bridge in 1989. Another big jump with about two hundred meters in span length was realized in the 1088m Sutong Bridge in 2008 and the 1104m Russky Bridge in 2012. Table 2 gives fifteen recording breaking cable-stayed bridges in the history [3].

No	Year	Bridge Name	Span(m)	Girder
1	1955	Strömsund	185	steel plate
2	1957	Theodor Heuss	284	steel box
3	1959	Severin	302	steel box
4	1969	Kniebrücke	319	steel box
5	1971	Duisburg-Neuenkamp	350	steel box
6	1974	Saint-Nazaire	404	steel box
7	1983	Barrios de Luna	440	PC box
8	1986	Alex Fraser	465	composite
9	1991	Iguchi	490	steel box
10	1991	Skarnsund	530	PC box
11	1993	Yangpu	602	composite
12	1995	Normandy	856	hybrid box
13	1999	Tatara	890	steel box
14	2008	Sutong	1,088	steel box
15	2012	Russky	1,104	steel box

Table 2. Record-breaking cable-stayed bridges.

As a human dream and an engineering challenge, the structural engineering of bridging larger obstacles has entered into a new era of crossing wide rivers and sea straits, including Tsugaru Strait in Japan, Qiongzhou Strait and Taiwan Strait in China, Sunda Strait in Indonesia, Messina Strait in Italy, Gibraltar Strait linking European and African Continents, and so on. One of the most challenging aspects has been identified as bridging capacity, for example, 1,500m span for Qiongzhou Strait, 2,016m for Sunda Strait and 5,000m for Taiwan Strait. With super long span length, cable-supported bridges are becoming lighter, more flexible, and lower damping, which result in more sensitive to wind actions, in particular wind resistance instability including aerodynamic flutter instability and aerostatic torsional divergence. Aerodynamic stabilization for cable-stayed bridges and suspension bridges have been firstly discussed in this paper, and followed by a new evaluation method, the robustness evaluation, for aerodynamic instability of cable-supported bridges [4].

Aerodynamic stabilization of cable-stayed bridges

Although the construction history of cable-stayed bridges has only about 62 years, cable-stayed bridge has become the most popular type of long-span bridges over the world for the past two to three decades. It is very interesting that almost all long-span cable-stayed bridges completed have suffered in rain and wind induced vibration (RWIV) of cables, which has been treated by either dimples or spiral wires on cable surfaces, sometimes together with dampers, but have had no other aerodynamic problem. The dynamic and aerodynamic performance of long-span cable-stayed bridges have been compared, and followed by some special countermeasures for aerodynamic flutter of longer spans in the near future.

Dynamic and aerodynamic performance of long-span cable-stayed bridges

In order to compare dynamic and aerodynamic performance of long-span cable-stayed bridges, the top five bridges except Russky Bridge have been selected, including 1,088m spanned Sutong Bridge, 1,018m Stonecutters Bridge, 926m Edong Bridge, 890m Tatara Bridge and 856m Normandy Bridge.

Sutong Bridge, connecting Suzhou City and Nantong City over Yangtze River in Eastern China, consists of seven steel deck spans including a 1088 m long central span. The cross-section of the deck is a streamlined orthotropic steel box, 35.4 m wide and 4 m deep, and carries three 3.75 m wide lanes of traffic in each direction with 3.5 m wide hard shoulders to provide an emergency parking zone shown in Fig. 1, which is quite similar to Tatara Bridge and Normandy Bridge. Stonecutters Bridge is composed of nine spans including a 1018m long central span. The cross-section of steel deck is twin streamlined orthotropic steel boxes, 2x15.9m wide and 3.9m deep, with three traffic lanes of 11m width in each direction and 3.3m wide hard shoulders for emergency parking shown in Fig. 2. Edong Bridge over Yangtze River is also a nine span hybrid cable-stayed bridge with a 926m long central span with steel deck. After having made the comparison of dynamic and aerodynamic characteristics with a traditional closed box, the cross-section of steel deck is designed as two separate box girder with the total deck width of 34.4m and the depth of 3.8m, without the bottom plate of a box at the central part to save steel material, shown in Fig. 3.

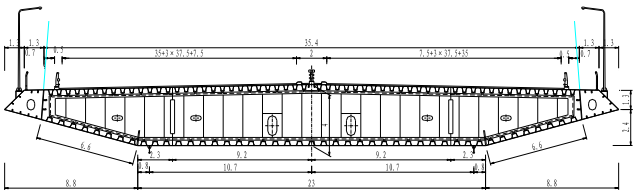

Figure 1. Deck cross-section of Sutong Bridge (Unit: m).

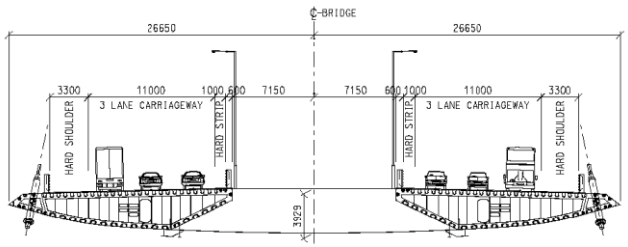

Figure 2. Deck cross-section of Stonecutters Bridge (Unit: mm).

The fundamental frequencies of lateral bending, vertical bending and torsion modes of these five cable-stayed bridges are listed and compared in Table 3. Among these five bridges, Tatara Bridge is an exceptional case always with the smallest values of the fundamental frequencies because of the least depth and width of the box girder, but with the largest ratio of the torsional frequency to the vertical frequency. With the unique twin box girder, Stonecutters Bridge has the next smallest fundamental frequencies of lateral and vertical bending modes, but almost the same torsional frequency as Tatara Bridge and Normandy Bridge. As the longest cable-stayed bridge, Sutong Bridge even has the higher torsional frequency than the other four bridges. It should be concluded that there is not any clear tendency that fundamental frequencies decrease with the increase of span length of cable-stayed bridges.

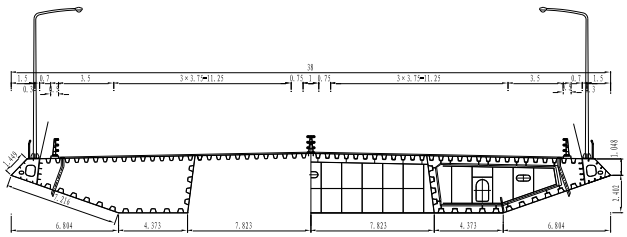

Figure 3. Deck cross-section of Edong Bridge (Unit: mm).

No	Bridge Name	Span (m)	Lateral (Hz)	Vertical (Hz)	Torsion (Hz)
1	Sutong	1,088	0.104	0.196	0.565
2	Stonecutters	1,018	0.090	0.184	0.505
3	Edong	926	0.153	0.235	0.548
4	Tatara	890	0.078	0.139	0.497
5	Normandy	856	0.151	0.222	0.500

Table 3. Fundamental frequencies of five long-span cable-stayed bridges.

The most important aerodynamic characteristic is flutter instability, which can be evaluated by simply comparing critical flutter speed with required wind speed. Critical flutter speed of a bridge can be determined through direct experimental method with sectional model or full aeroelastic model and computational method with experimentally identified flutter derivatives, and required wind speed is based on basic design wind speed multiplied by some modification factors. Both the critical flutter speeds and the required wind speeds of these five bridges are shown in Table 4. It is very surprised to see that both critical flutter speeds and required wind speeds steadily increase with the increase of main span, and may support to make another jump in span length of cable-stayed bridges in the near future [4].

No	Bridge Name	Span (m)	Freq. ratio	Flutter (m/s)	Required (m/s)
1	Sutong	1,088	2.88	88.4	71.6
2	Stonecutters	1,018	2.74	140	79.0
3	Edong	926	2.33	81.0	58.6
4	Tatara	890	3.58	80.0	61.0
5	Normandy	856	2.25	78.0	58.3

Table 4. Aerodynamic stability of five long-span cable-stayed bridges.

Special countermeasures for aerodynamic flutter of longer spans

Some special countermeasures for aerodynamic stabilization have been experimentally investigated for a cable-stayed bridge with single 1,400m span shown in Fig. 4. The fundamental natural frequencies of the lateral bending, the vertical bending and the torsional vibration of bridge deck obtained via a FEM modal analysis are 0.0611Hz, 0.1474Hz and 0.4157Hz, respectively, and the corresponding modal equivalent masses and mass moment of the bridge deck are 29,087 kg/m, 32,894 kg/m and 4,606,300 kgm^2/m, respectively [5].

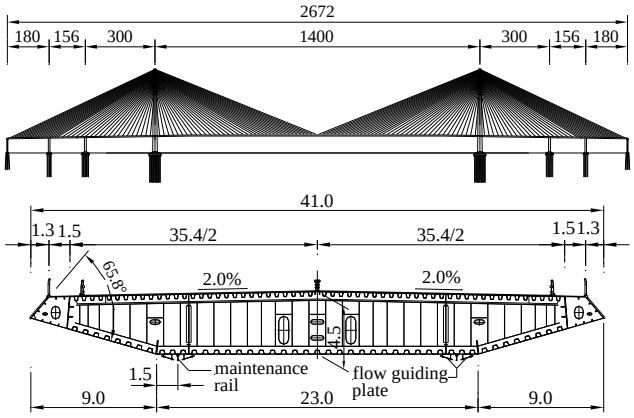

Figure 4. Single 1,400m span cable-stayed bridge (unit: m).

The wind tunnel tests of sectional models were firstly conducted on the original deck under smooth flow for three wind attack angles of +3°, 0° and -3°. The corresponding tested flutter critical wind speeds are 58m/s, 104m/s and >110m/s, respectively, and the lowest critical wind speed of 58m/s is much smaller than the desired flutter checking speed of 80m/s. The further experiments were put on four kinds of aerodynamic countermeasures, including the upper central stabilization plate (UCSP) with the height of 1.5m, the combination of the upper and lower central stabilization plate (ULCSP) with the both heights of 1.5m, the cantilever horizontal stabilization plate (CHSP) at the nose tips of both wind fairings with the widths of 1.0m, 1.2m, 1.5m, 1.7m and 2.0m, and the central slotting (CS) with the gap widths of 0.1B, 0.15B and 0.2B, shown in Fig. 5. The general testing results indicate that both the UCSP and ULCSP measures play little influence on the flutter performance, and the measures of CS exerts negative effect on the flutter performance of the bridge when the gap width is below 0.15B, and can raise the flutter critical wind speed up to 74m/s (28%) when the gap width increases to 0.2B, but it is still below 80m/s. The most effective counter measure is the CHSP with the optimal width of 1.5m, by which the flutter critical speed can be significantly raised from 58m/s to 110m under +3°, slightly decreases from 104m/s to 96m/s under 0°, and keeps greater than 110m/s under -3°[5].

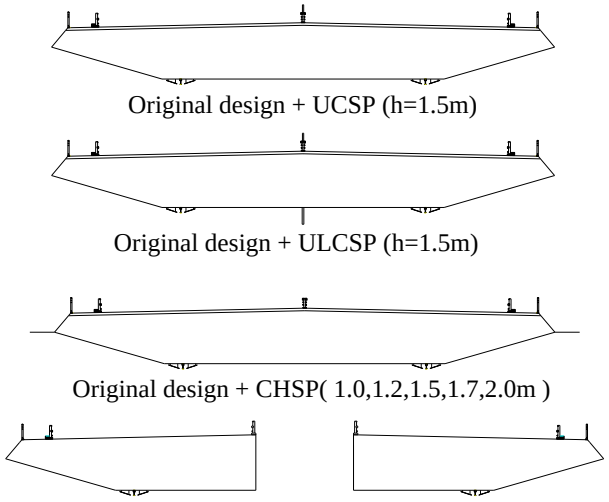

Figure 5. Four kinds of aerodynamic countermeasures.

It should be noted that the flutter critical speeds obtained via full bridge aeroelastic model testing are evidently lower than those gained via sectional model testing by 10~20%, and the vibration mode approaching flutter of the bridge deck showed a strong coupling behaviour not only in the torsional and vertical degrees, but also in the lateral degree. However, the mechanisms of how the above-mentioned factors advance the onset points of the static and dynamic instabilities is not clear yet and needs to be further investigated [5].

Feasible stabilizing longer double main-span cable-stayed bridge

The double 1,500m spans cable-stayed bridge has been proposed for the main navigational channel of Qiongzhou Strait Bridge in China. The span arrangement was designed with six spans, 244 + 408 + 1500 + 1500 + 408 + 244 m, and the twin box deck was adopted with the total width of 60.5m including a 14m central slot, shown in Fig. 6. The fundamental natural frequencies of the lateral bending, the vertical bending and the torsional vibration of bridge deck obtained via a FEM modal analysis are 0.0810Hz, 0.1235Hz and 0.3524Hz, respectively, and the corresponding modal equivalent masses and mass moment of the bridge deck are 39,020 kg/m, 54,370 kg/m and 15,699,500 kgm^2/m, respectively [6].

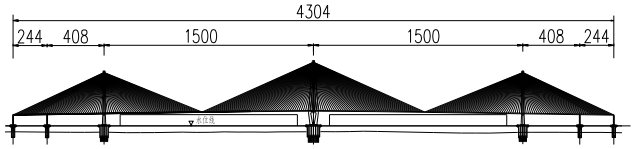

(a) General span arrangement (unit: m).

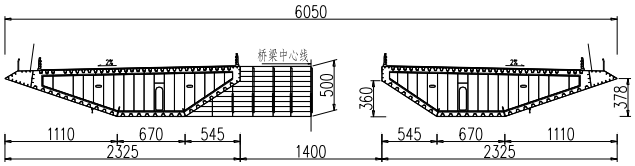

(b) Deck cross section (unit: mm).

Figure 6. Double 1,500m spans cable-stayed bridge.

The flutter performance of the bridge was firstly studied through wind tunnel testing with a 1:80 sectional model under smooth flows at three wind attack angles of +3°, 0° and -3°. The corresponding tested flutter critical wind speeds are all over 118m/s, which is much larger than the desired flutter checking speed of 93m/s for this typhoon prone area [6].

In order to investigate the three-dimensional effect of bridge deformation and vibration on aerodynamic flutter instability and aerostatic torsional divergence, which was raised by the previous 1,400m spanned cable-stayed bridge, the further wind tunnel testing with a 1:320 full bridge aeroelastic model was carefully conducted under smooth flows at the wind attack angles of +3°, 0° and -3°. The corresponding critical wind speeds for aerostatic torsional divergence are smaller than those due to aerodynamic flutter instability, which means that the structural resistance to wind-induced aerodynamic and aerostatic instabilities of such a long cable-stayed bridge with a twin box deck becomes very close to each other. This phenomenon together with the interaction between these two kinds of instabilities should be seriously taken into account in the future design [6].

Effective stabilization of suspension bridges

Top ten longest-span suspension bridges completed in the world are listed in Table 5 [7], and seven of them have encountered aerodynamic problems including five in flutter and two in vortex induced vibration (VIV). Both Great Belt Bridge and the 4th Nanjing Bridge have simply used guide vanes to improve VIV, and the other five bridges suffered in flutter have adopted three kinds of control measures, including stabilizer, slot or twin-box and their combination, which are discussed as effective stabilization.

No	Bridge Name	Span (m)	Girder Type	Wind Problem	Control Measure
1	Akashi Kaikyo	1,991	Truss	Flutter	Slot/ Stabilizer
2	Xihoumen	1,650	Box	Flutter	Twin box
3	Great Belt	1,624	Box	VIV	Guide vane
4	Yi Sun-sen	1,545	Box	Flutter	Twin box
5	Runyang	1,490	Box	Flutter	Stabilizer
6	4th Nanjing	1,418	Box	VIV	Guide vane
7	Humber	1,410	Box	No	None
8	Jiangyin	1,385	Box	No	None
9	Tsing Ma	1,377	B/T	Flutter	Slot
10	Hardanger	1,310	Box	No	None

Table 5. Top ten longest-span suspension bridges completed in the world.

Stabilizer on single box girder

Among the top ten suspension bridges in Table 5, Runyang Bridge across Yangtze River in China completed in 2005 is the second longest suspension bridge in China and the fifth longest in the world. The main section of the bridge was designed as a typical three-span suspension bridge with the span arrangement of 510m + 1490m + 510m and the deck cross section of 36.3m width and 3m depth shown in Fig. 7.

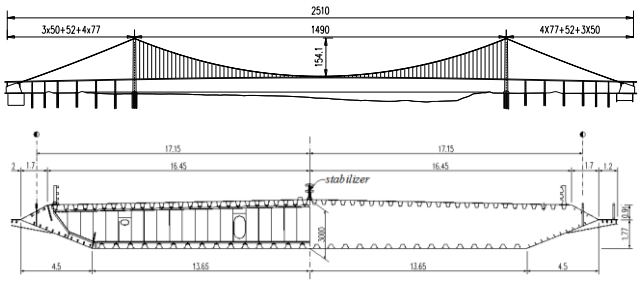

Figure 7. Runyang Bridge across Yangtze River (Unit: m).

In order to investigate aerodynamic flutter, a wind tunnel experiment with a 1:70 sectional model was carried out. It was found in the first phase of the testing that the original structure could not meet the requirement of checking flutter speed of 54m/s. Some preventive means had to be considered to stabilize the original structure. With a stabilizer in the centre of the bridge deck, further sectional model testing was conducted, and the confirmation wind tunnel tests with a full aeroelastic model were also performed. The critical flutter speeds obtained from the sectional model (SM) and the full model (FM) wind tunnel tests are collected and compared in Table 6, and the central stabilizer of 0.88 m height as shown in Fig. 8 can raise the critical flutter speed over the required value [8].

Figure 8. Stabilizer mounted on Runyang Bridge.

Deck	Critical flutter speed (m/s)				Required
	0° SM	0° FM	3° SM	3° FM	(m/s)
No Stab.	64.4	64.3	50.8	52.5	54
0.65m Stab.		69.5	58.1	53.8	54
0.88m Stab.		72.1	64.9	55.1	54
1.10m Stab.		>75	67.4	56.4	54

Table 6. Critical flutter speed of Runyang Bridge.

Slot in twin-box girder

Xihoumen Bridge route is selected at the shortest distance of the Xihoumen Strait between Jintang Island and Cezi Island in China, about 2200 m far away. Between these two islands and near Cezi, there is a small island, called Tiger Island, which can be used to hold on a pylon for a cable-supported bridge. In order to avoid from constructing deep-water foundation, Xihoumen Bridge is designed as a two-continuous-span suspension bridge with the span arrangement of 578m + 1650m + 485m shown in Fig. 9.

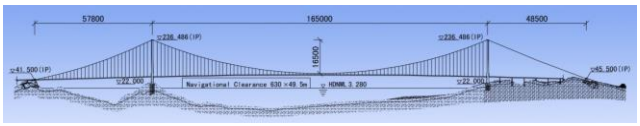

Figure 9. Longitudinal arrangement of Xihoumen Bridge (Unit: cm).

Based on the experience gained from the 1,490m Runyang Bridge with critical flutter speed of 51 m/s and the 1624 m Great Belt Bridge with 65 m/s critical speed, the span length of 1650 m may suffer with aerodynamic instability for suspension bridges, even with the stricter stability requirement of 78.4 m/s in Xihoumen Bridge located in typhoon prone area. Besides traditional single box girder and the box girder with a central stabilizer, two more twin box girders with a central slot of 6m and 10.6m, were investigated through sectional model wind tunnel testing. The experimental results of critical flutter speeds are summarized for these four cross section girders in Table 7. Apart from the traditional single box, the rest three cross sections can meet with the flutter stability requirement. The twin box girder with a 6m slot was finally selected as the proposed scheme, which was further modified to the final configuration as shown in Fig. 10 [9]. Twin box girder has been firstly adopted for the purpose of aerodynamic stabilization in Xihoumen Bridge in China in 2009, and followed by Yi Sun-sen Bridge in Korea in 2012.

Deck	Critical flutter speed (m/s)				Required
	–3°	0°	+3°	Min.	(m/s)
Single box	50.7	46.2	48.7	46.2	78.4
2.2m Stab.	>89.3	>89.3	88.0	88.0	78.4
Twin-box with 6m slot	88.4	>89.3	>89.3	88.4	78.4
Twin-box with 10.6m	>89.3	>89.3	>89.3	>89.3	78.4

Table 7. Critical flutter speeds of Xihoumen Bridge.

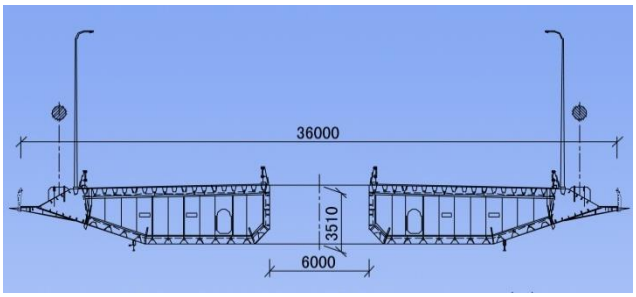

Figure 10. Twin box girder of Xihoumen Bridge.

Combination of slot and stabilizer

The span arrangement of Akashi Kaikyo Bridge is set as 960m + 1991m + 960m, the longest central span of suspension bridges. According to the Japanese code, the checking flutter speed is set to 78m/s considering the local wind environment. This makes it a severe problem to design an appropriate stiffening girder, whose aerodynamic stability must be good enough to satisfy the required checking wind speed, with such an extremely flexible structure. Substantial efforts had been made to optimize the aerodynamic shape of the girder. Several girder types were examined by sectional model and also numerical analysis, shown in Fig. 11 [10].

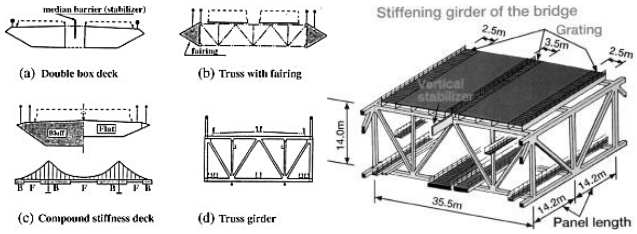

Figure 11. Aerodynamic optimization of the bridge's deck.

Truss girder with central stabilizer and slotting was finally selected, shown in Fig. 11, due to both the wind-resistant requirement and the erection process. On one hand, a simple truss girder without any control measures cannot provide sufficient stability under the checking wind speed. Installation of a vertical stabilizer upon the upper road deck and slotting of the lower road deck were found to be necessary. On the other hand, it is convenient to introduce the cantilever erection method. The girder can be constructed starting from the tower without interrupting the sea traffic, rather than lifting the girder block from the navigation channel if steel box girder were used [11].

As a final check of the overall flutter stability of the bridge structure, wind tunnel tests with a full aeroelastic model were carried out. The involved three-dimensional characters were thus considered, like the varying torsional deflection along the bridge axis, the spatial correlation of the wind field, and the interference between the cables and the girder, et al. It was found that the stabilizer could be restricted to the centre span only, giving a much more economical solution. At that time, it also provided evidences of the accuracy of numerical calculation, helping the Finite-Element-Method (FEM) widely used in flutter analysis nowadays.

Challenging stabilization of longer suspension bridges

Five longer span suspension bridges proposed in the world are listed in Table 8, with a steel box or truss girder span from 1666m to 5000m under feasibility study, working design or bridge construction.

No	Bridge Name	Span (m)	Girder Type	Wind Problem	Control Measure
1	Lingding Channel	1,666	Box	Flutter	V/H Stabilizer
2	2nd Humen	1,688	Box	Flutter	Horizontal Stabilizer
3	Shuangyumen	1,756	Box	Flutter	Twin Box
4	Sunda Strait	2,016	B/T	Flutter	Twin Box
5	Taiwan Strait	5,000	Box	Flutter	Twin Box

Table 8. Longer span suspension bridges under construction or design.

All five suspension bridges have encountered aerodynamic flutter problems. Three kinds of flutter countermeasures, including horizontal stabilizers, combination of vertical and horizontal stabilizers and twin/triple boxes, have been investigated through wind tunnel tests for engineering applications [4].

Horizontal stabilizers on single box girder

The 2nd Humen Bridge across Pearls River in China was designed as a suspension bridge with a main span of 1,688m and a deck width for 8 traffic lanes shown in Fig. 12, and began to be constructed in 2015. Since the original single box girder could not meet with the required flutter checking speed of 63.3m/s, two possible horizontal stabilizers with 1.5m width and 2.5m width, had been tried through wind tunnel tests.

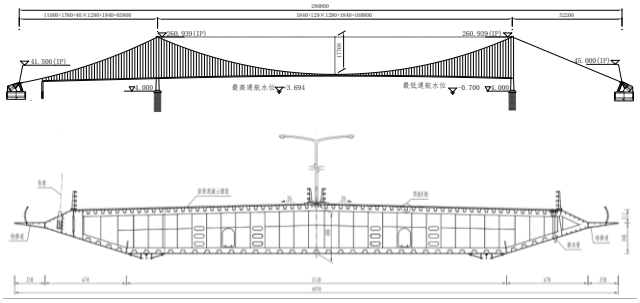

Figure 12. The 2nd Humen Bridge (Unit: cm).

The experimental results of critical flutter speeds through the sectional model (SM) and the full model (FM) are summarized for these three cross section girders, including 0m, 1.5m and 2.5m wide horizontal stabilizers, in Table 9. Although the critical flutter speeds of the full model testing are smaller than those of the sectional model testing, the horizontal stabilizers with 2.5m width can meet with the required flutter checking speed of 63.3m/s. The single box girder with 2.5m wide horizontal stabilizers has been finally selected as the proposed scheme [12].

Horizontal Stabilizers	Critical flutter speed (m/s)				Required
	–3°	0°	+3°	Min.	(m/s)
0.0 m (SM)	83.5	56.7	55.7	55.7	63.3
1.5 m (SM)	83.5	76.0	58.6	58.6	63.3
2.5 m (SM)	77.7	77.9	82.5	77.7	63.3
2.5 m (FM)	76.2	71.7	70.7	70.7	63.3

Table 9. Critical flutter speeds of the 2nd Humen Bridge.

Combination of vertical and horizontal stabilizers on single box girder

About 30km down steam of the 2nd Humen Bridge along Pearls River, the Lingding Channel Bridge was also preliminarily designed as a suspension bridge, with a main span of 1,666m and a deck width for 8 traffic lanes shown in Fig. 12, and will begin to be built at the end of 2017. Since the required flutter checking speed of this bridge is 83.7m/s, about 20/s higher than that of the 2nd Humen Bridge, the 2.5m wide horizontal stabilizers cannot meet with the requirement. The combination of vertical and horizontal stabilizers has been tested with sectional models shown in Fig. 13.

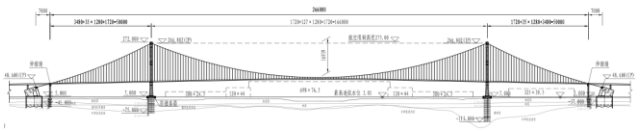

Figure 12. Lingding Channel Bridge (Unit: cm).

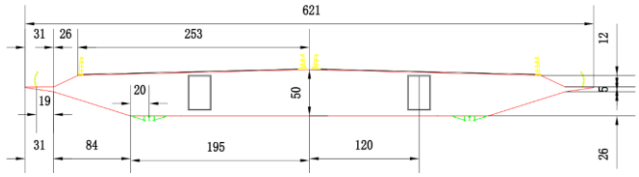

Figure 13. 1:80 Sectional model of Lingding Channel Bridge (Unit: mm).

The critical flutter speeds due to the sectional model tests are summarized for three combinations of vertical and horizontal stabilizers, including 1.2m up, 0.8m down and 1.2m up plus 0.8m down vertical stabilizers, in Table 10. Although the minimum critical flutter speed of the last combination scheme is 84.0m/s, which is greater than the requirement of 83.7m/s, the safety margin is not large enough to overcome the difference between sectional model testing and full model testing. The depth of the single box girder has been proposed to increase from 4m to 5m, and the minimum critical flutter speed has been raised to 87m/s. It is necessary to confirm this result by full aeroelastic model testing in the next step [13].

Vertical Stabilizers	Critical flutter speed (m/s)				Required
	–3°	0°	+3°	Min.	(m/s)
Without	77.7	77.9	82.5	77.7	83.7
1.2m Up	83.0	90.0	83.5	83.5	83.7
0.8m Down	80.5	82.9	81.7	81.7	83.7
1.2m up plus 0.8m down	87.5	92.5	84.0	84.0	83.7

Table 10. Critical flutter speeds of Lingding Channel Bridge.

Further optimization of twin box girder

With the increase of span length and required flutter checking speed of suspension bridges, vertical stabilizer, horizontal stabilizers and their combination mounted on single box girder may not be enough to guarantee aerodynamic flutter stability, and twin box girder could be a better choice. In order to further optimize twin box girder after Xihoumen Bridge and Yi Sun-sen Bridge, three proposed super-long span suspension bridges with twin box girder will be discussed in this section.

Located in the Zhoushan Archipelago in China, Shuangyumen Bridge was preliminarily designed as a suspension bridge with a single span of 1,708m and a deck width for only 4 traffic lanes. Due to the adverse wind environment at the bridge site, the required flutter checking wind speed is 80m/s, and two possible girder schemes were proposed, single box girder with the combination of vertical and horizontal stabilizers and twin box girder, shown in Fig. 14. As far as flutter performance is concerned, twin box girder is a better solution compared with single box girder even with the combination of vertical and horizontal stabilizers. In this investigation, the slotting width ratio, b/B, and the chamfering size, hxd, of the inner corner were selected as shape optimization parameters, the results from sectional model wind tunnel tests are listed in Table 11. the flutter performance is improved by the increasing of slot width ratio as the chamfering size of inner corner is fixed to hxd = 0.9×0.9m, while the enlarging of inner corner chamfering will also increase the flutter critical wind speed. All five cases have critical wind speed higher than 89.6m/s, which suggests that central slot has certain superiority in flutter control domain [14].

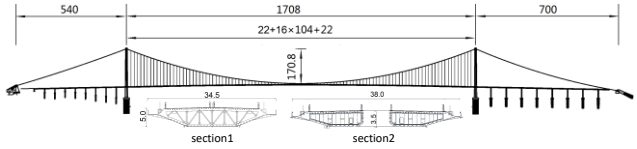

Figure 14. Design scheme of Shuangyumen Bridge (Unit: m).

b / B (m/m)	h x d (mxm)	Critical flutter speed (m/s)			
		–3°	0°	+3°	Min.
5 / 37	0.9×0.9	89.6	>100	>100	89.6
5.5 / 37.5	0.9×0.9	91.8	>100	>100	91.8
6 / 38	0.9×0.9	92.4	>100	>100	92.4
6 / 38	2.3×2.3	94.1	>100	>100	94.1
6 / 38	4.7×2.3	95.2	>100	>100	95.2

Table 11. Critical flutter speeds of Shuangyumen Bridge.

As a main part of the Trans Asian & Asean Highway and Railway in Indonesia, Sunda Strait Bridge linking Sumatra Island and Java Island is planned as a super-long span suspension bridge with the span arrangement of 792+2016+792m and the cable sag to span ratio of 1/10 as shown Fig. 15. In the conceptual design stage, there are two stiffening girder design schemes provided by the designers, that is, the deep twin box girder and the shallow twin box girder in Fig. 15. The deep twin box girder is 51.8m wide and 9.76m deep with a central slot width of 2.25m, and the shallow one is 60.35m wide and 5.8m deep with a slot of 10.8m. The ventilation ratios of these two girders can be calculated by dividing net slot area by total slot area, and have the values of 31% in the deep scheme and 53% in the shallow scheme, respectively, which are very important to aerodynamic flutter stability.

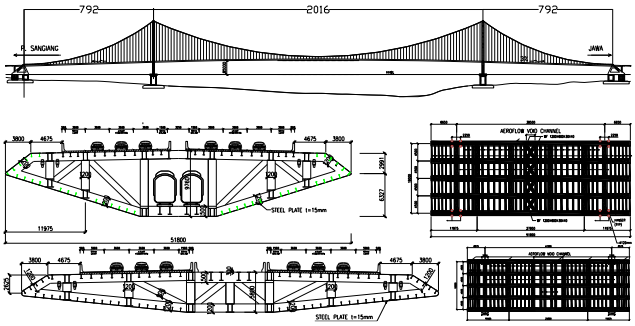

Figure 15. Design scheme of Sunda Strait Bridge (Unit: m).

The experimental results of the flutter critical wind speeds with different angles of attack are listed and compared in Table 12. The minimum flutter critical speed is 82m/s for the deep twin box girder scheme and 93m/s for the shallow twin box girder scheme, respectively. Since the flutter checking speed of Sunda Strait Bridge is set to 93m/s, the aerodynamic flutter stability performance of both design schemes may need to be further improved in the next design stage. It is suggested that the further improvement can be realized by either increasing the width or ventilation ratio of central slot or adopting additional central stabilizer like the combination of stabilizer and slot in Akashi Kaikyo Bridge [15].

Twin box girder	Critical flutter speed (m/s)				Required
	–3°	0°	+3°	Min.	(m/s)
Deep	84	87	82	82	93
Shallow	93	108	113	93	93

Table 12. Critical flutter speeds of Sunda Strait Bridge.

With the emphasis on aerodynamic stabilization for super-long span length, a typical three-span suspension bridge with a 5,000m central span and two 1,600m side spans is considered for Taiwan Strait as shown in Fig. 16. Two kinds of generic deck sections, namely a widely slotted deck (WS) without any stabilizers (Fig. 17a) and a narrowly slotted deck with vertical and horizontal stabilizers (NS) (Fig. 17b), were investigated. The WS cross section has a total deck width of 80m and four main cables for a 5,000m-span suspension bridge while the NS provides a narrower deck solution of 50m and two main cables [16][17].

Figure 16. Span arrangement Taiwan Strait Bridge (Unit: m).

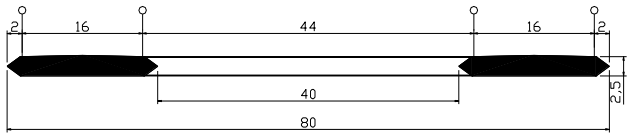

a) Widely slotted deck (WS).

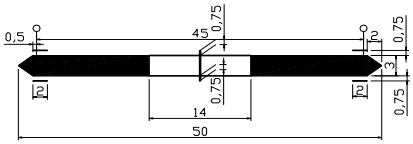

a) Narrowly slotted deck (NS).

Figure 17. Two kinds of generic deck sections (Unit: m).

The results of critical wind speeds are summarized in Table 13. For both deck sections the critical wind speed increases with decrease of the ratio n, although the frequency ratio of torsion to vertical bending slightly decreases. The most important reason is the considerable increase of the generalized properties in the aerodynamic stability analysis. The minimum critical wind speeds for the WS and NS sections are 82.9 m/s and 74.7 m/s, respectively [17][18].

Ratio	f_h (Hz)		f_α (Hz)		U_{cr} (m/s)	
	WS	NS	WS	NS	WS	NS
n = 1/8	0.0596	0.0594	0.0709	0.0907	82.9	74.7
n = 1/9	0.0613	0.0612	0.0721	0.0893	88.8	77.4
n = 1/10	0.0622	0.0620	0.0727	0.0865	90.9	78.9
n = 1/11	0.0624	0.0622	0.0727	0.0840	98.9	82.7

Table 13. Critical flutter speeds of Taiwan Strait Bridge.

Robustness evaluation of aerodynamic stabilization

Probabilistic model for robustness evaluation

There are two methods and indexes often adopted to evaluate the wind-resistance performance of long span bridges, including the safety coefficient based on the allowable stress method and the partial coefficient based on the ultimate limit state method.

The safety coefficient based on the allowable stress method can be defined as follows

$$K = \frac{U_{re}}{U_{ac}} \tag{1}$$

where U_{re} is the wind speed that the bridge resists, and U_{ac} is the maximum design wind speed. The bridge is safe when the K coefficient is larger than 1. The larger the coefficient K is, the safer the bridge will be. On the contrary, the bridge will fail when the coefficient K is smaller than 1.

For the ultimate limit state method, the safety factor is considered as the partial coefficient and directly expressed in the equation of ultimate limit state. Take the evaluation of flutter stability as an example, the safety of wind-resistance can be expressed as

$$K_1 U_{re} \geq K_2 U_{ac} \tag{2}$$

where K_1 is the partial coefficient for the wind speed that the bridge resists and K_2 is the partial coefficient for the maximum design wind speed.

Considering the definition given by Knoll and Vogel [19] and taking into account the maximum wind speed that is unforeseen during the design stage, the definition of wind resistance robustness of bridges could be given as the ability that the bridge possesses to resist the maximum wind speed which is beyond common situation. It is represented by the return period T_m of the design wind speed U_{ac} and is expressed as

$$T_m = \frac{1}{P_F} \tag{3}$$

where P_F is the failure probability for the wind resistance of bridge structure, which could be calculated as

$$P_F = P\{Z \leq 0\} \tag{4}$$

where Z is the random function of the safety domain, based on the fundamental variables U_{re} and U_{ac}. When T_m is shorter than the design service life of the bridge (i.e. 100 years), the wind resistance ability of the bridge could not meet the requirement. On the contrary, the wind resistance ability of the bridge is enough when T_m is longer than the design service life of the bridge. The return period T is not only an intuitive index for evaluating the wind resistance performance, but also an index which could be easily compared with other disaster factors (i.e. earthquake, fire, collision, and etc.).

The wind-resistance performance of bridges consists of the strength, the stiffness and the stability of the bridge. The strength robustness of bridge wind-resistance consists of the robustness of static wind load and the dynamic wind load. The stiffness robustness of bridge wind-resistance consists of the stiffness robustness of vortex vibration and buffeting. On condition that there has been no reasonable limit on the vortex vibration and buffeting stiffness of long-span bridges by far, the stiffness robustness of bridge wind-resistance would be evaluated by the robustness of comfort degree. The stability robustness of bridge wind-resistance consists of static stability and dynamic stability, including static torsional divergence, overall lateral buckling and dynamic flutter instability under extreme wind speed.

As part of the wind-resistance performance of bridges, flutter robustness could be calculated by Eqs. (3) and (4) as are introduced above. The random function of safety domain in Eq. (4), therefore, needs to be defined.

In the evaluation of the bridge flutter performance, the wind speed that the bridge resists U_{re} is given by the multiply of the critical flutter wind speed U_f by the corresponding correction coefficient C_f

$$U_{re} = C_f U_f \tag{5}$$

where both C_f and U_f are random variables. The maximum design wind speed U_{ac} is given by the multiply of the design standard wind speed U_b by the corresponding correction coefficient C_b

$$U_{ac} = C_b U_b \tag{6}$$

where C_b and U_b are random variables.

The random function of safety domain could be given by the function of the four fundamental variables introduced above

$$Z = g(X_1, X_2, X_3, X_4) = g(C_f, U_f, C_b, U_b)$$

$$= \frac{C_f}{C_b} U_f - U_b \tag{7}$$

where $g(X)$ is the joint probability density function of the four fundamental variables. In theory, the return period T_m could be obtained from Eq. (3) by substituting Eq. (7) into Eq. (4). In reality, however, it would be too difficult to obtain the failure probability P_F in this way. The calculation of the failure probability will be conducted by the equivalent central point method as well as the equivalent checking point method.

Robustness parameter calculation approaches

The critical flutter wind speed U_f is mainly determined by the mass, stiffness and damping of the structure and is a random variable which could partially reflect the structural behavior of the bridges. According to Ge [20], U_f could be assumed to follow lognormal distribution and the mean value and standard deviation could be conservatively defined as

$$E\left[U_f\right]=\mu_{U_f} \tag{8}$$

$$\sigma\left[U_f\right]=\sigma_{U_f}=0.075\mu_{U_f} \tag{9}$$

where μ_{U_f} is the mean value of critical flutter speed based on wind tunnel experiments or numerical analysis.

The correction coefficient of critical flutter speed C_f is largely influenced by the uncertain difference between the wind speed in experimental model test and the wind speed in field measurement. The comparison between these two kinds of wind speed indicates that the correction coefficient has large fluctuation [21]. In order to simplify the calculation process, the coefficient C_f is assumed to distribute normally with the mean value 1.0 and standard deviation 5%.

$$E\left[C_f\right]=\mu_{C_f}=1.0 \tag{10}$$

$$\sigma\left[C_f\right]=\sigma_{C_f}=0.05 \tag{11}$$

The design standard wind speed U_b at the bridge deck is usually assumed to follow extreme value distribution. In Chinese *Wind-resistant Design Specification for Highway Bridges* [22], it is stipulated that U_b follows extreme value distribution-I, of which the probability distribution function is

$$F(U_b)=\exp\left[-\exp\left(-\frac{U_b-b}{a}\right)\right] \tag{12}$$

where a and b are variables related to the deviation and location, respectively, and can be given as

$$E\left[U_b\right]=\mu_{U_b}=0.5772a+b \tag{13}$$

$$\sigma\left[U_b\right]=\sigma_{U_b}=\frac{\pi}{\sqrt{6}}a \tag{14}$$

The correction coefficient C_b mainly concerns modification for the gust factor. According to Ge [20], C_b is assumed to distribute normally and its mean value and standard deviation are conservatively defined as

$$E\left[C_b\right]=\mu_{C_b} \tag{15}$$

$$\sigma\left[C_b\right]=\sigma_{C_b}=0.07\mu_{C_b} \tag{16}$$

where the value of μ_{C_b} is stipulated in Chinese Specification [22].

Among the four fundamental variables of random function of safety domain $Z = g(X)$, U_f and U_b are not normally distributed, and thus they need to be transformed into standard normal variables X_2 and X_4 [23]. To do so, the mean value and standard deviation of the equivalent normal variable need to be calculated at the calculating point $X=(X_1, X_2, X_3, X_4)$

$$\mu'_{X_i}=X'_i-\Phi^{-1}\left[F_{X_i}(X'_i)\right]\sigma'_{X_i} \tag{17}$$

$$\sigma'_{X_i}=\frac{\varphi\left\{\Phi^{-1}\left[F_{X_i}(X'_i)\right]\right\}}{f_{X_i}(X'_i)} \tag{18}$$

where $\Phi(\cdot)$ and $\varphi(\cdot)$ are standard normal distribution function and density function, respectively. $F_{Xi}(\cdot)$ and $f_{Xi}(\cdot)$ are the distribution function and destiny function of fundamental variables. Even though fundamental variables C_f and C_b are normally distributed, they still need to be transformed into standard normal variables X_1 and X_3.

For linear random function of safety domain Z and normally distributed fundamental variables, failure probability P_F and reliability index β have following relationships

$$P_F=\Phi(-\beta)\Leftrightarrow\beta=-\Phi^{-1}(P_F) \tag{19}$$

$$\beta=\frac{\mu_Z}{\sigma_Z} \tag{20}$$

where μ_z and σ_z are the mean value and standard deviation of Z, respectively. And $\Phi(\cdot)$ is standard normal distribution function.

Safety domain Z for arbitrary fundamental variables $X=(X_1, X_2, \cdots, X_n)$ and its Taylor expansion formula at $(X_1, X_2, \cdots, X_n)=(\mu_1, \mu_2, \ldots, \mu_n)$ could be derived as

$$Z=f(X)=f(X_1,X_2,\cdots,X_n)$$

$$\cong f(\mu_1,\mu_2,\cdots,\mu_n)+\sum_{i=1}^{n}\frac{\partial f}{\partial X_i}(X_i-\mu_i) \tag{21}$$

where $\partial f/\partial X_i$ is calculated at point $(\mu_1,\mu_2,\cdots,\mu_n)$. From Eq. (21), the approximate values of μ_z and σ_z could be expressed as

$$\mu_Z\cong f(\mu_1,\mu_2,\cdots,\mu_n) \tag{22}$$

$$\sigma_Z^2\cong\sum_{i=1}^{n}\sum_{j=1}^{n}\frac{\partial f}{\partial X_i}\frac{\partial f}{\partial X_j}Cov\left[X_i,X_j\right] \tag{23}$$

Assuming that the fundamental variables $X=(C_f, U_f, C_b, U_b)$ are independent, the reliability index β based on the equivalent central point method (ECPM) could be calculated.

Since the random function of safety domain $Z = g(X)$ for the four fundamental variables is nonlinear, Z needs to be expanded at the checking point $P^*(\mu'^*_{X1}, \mu'^*_{X2}, \mu'^*_{X3}, \mu'^*_{X4})$ [24]

$$Z=g(X)=g\left(\mu'_{X_1}\sigma_{X_1}+\mu_{X_1},\mu'_{X_2}\sigma_{X_2}+\mu_{X_2},\right.$$

$$\left.\mu'_{X_3}\sigma_{X_3}+\mu_{X_3},\mu'_{X_4}\sigma_{X_4}+\mu_{X_4}\right)$$

$$+\sum_{i=1}^{4}\left(\frac{\partial g}{\partial \mu'_{X_i}}\right)_{P^*}\left(\mu'_{X_i}-\mu'^{*}_{X_i}\right) \tag{24}$$

Assuming that the fundamental variables $X=(C_f, U_f, C_b, U_b)$ are independent, the flutter reliability index β based on the equivalent checking point method would therefore, be determined by the following five equations [25]

$$\alpha_i=\frac{-\dfrac{\partial g(\beta\alpha)}{\partial \mu'_{X_i}}}{\sqrt{\sum_{k=1}^{4}\left[\dfrac{\partial g(\beta\alpha)}{\partial \mu'_{X_k}}\right]^2}}, i=1,2,3,4 \tag{25}$$

$$g(\beta\alpha_1,\beta\alpha_2,\beta\alpha_3,\beta\alpha_4)=0 \tag{26}$$

where $\alpha=(\alpha_1,\alpha_2,\cdots,\alpha_n)$ is a unit vector.

The reliability index β would be obtained by iteratively calculating the five equations above.

Robustness evaluation of aerodynamic stability

In order to analyze and compare flutter robustness, four completed long-span bridges, including Nanpu Bridge, Yangpu Bridge, Runyang Bridge and Xihoumen Bridge, have been taken as examples. The mean value and standard deviation of four fundamental random variables of these four bridges are listed in Table 14. For the Nanpu Bridge and Yangpu Bridge in Shanghai, the mean value μ_{ac} and standard deviation σ_{ac} of the design standard wind speed recorded by meteorological monitoring station (Load case I) and adopted in the design procedure (Load case II) are both listed in the table. The two bridges have identical values so as to make comparisons. For the other two bridges, only the mean value μ_{ac} and standard deviation σ_{ac} of the design standard wind speed adopted in the design procedure (Load case II) are listed.

Bridge Name	Nanpu		Yangpu		Runyang	Xihoumen
Situation	I	II	I	II	II	II
μ_{K1}	1	1	1	1	1	1
σ_{K1}	0.05	0.05	0.05	0.05	0.05	0.05
μ_{re}	66.4	66.4	83.5	83.5	55.1	88.4
σ_{re}	5.00	5.00	6.30	6.30	4.10	6.6
μ_{K2}	1.34	1.34	1.32	1.32	1.22	1.22
σ_{K2}	0.09	0.09	0.09	0.09	0.09	0.09
μ_{ac}	17.6	20.8	17.6	20.8	22.7	33.1
σ_{ac}	3.18	4.17	3.18	4.17	4.54	6.62

Table 14. Mean values and standard deviations of fundamental variables for four completed bridges.

Based on equivalent central point method and equivalent checking point method, the robustness evaluation of flutter stability for these four bridges are conducted, and the calculation results are summarized in Table 15 and Table 16. Having made comparison of reliability index β between two methods, there is only about 1.1% to 2.4% difference in values of β, and the equivalent central point method is recommended for its simplicity.

After the analysis of the four completed long-span bridges, the robustness evaluation has also been applied on other four proposed super long span suspension bridges previously mentioned, the 2nd Humen Bridge, Linding Channel Bridge, Shuangyumen Bridge and Sunda Strait Bridge. The statistic characteristics of the fundamental random variables of those four bridges are listed in Table 17. Based on the equivalent central point method and the equivalent checking point method, the reliability index, failure probability and return period calculated are listed and compared in Table 18.

Bridge Name	Situation	β_0	P_{F0}	T_{ac0}
Nanpu	I	4.1838	1.43e-05	69776
	II	3.4223	3.11e-04	3220
Yangpu	I	5.0311	2.44e-07	4100756
	II	4.2398	1.12e-05	89390
Runyang	II	2.7953	2.59e-03	386
Xihoumen	II	3.1173	9.13e-04	1096

Table 15. Robustness evaluation of flutter stability for four completed bridges based on the equivalent central point method.

Bridge Name	Situation	β_1	P_{F1}	T_{ac1}
Nanpu	I	4.2582	1.03e-05	97038
	II	3.4611	2.69e-04	3718
Yangpu	I	5.1523	1.29e-07	7771000
	II	4.3106	8.14e-06	122860
Runyang	II	2.8271	2.35e-03	426
Xihoumen	II	3.1581	7.94e-04	1259

Table 16. Robustness evaluation of flutter stability for four completed bridges based on the equivalent checking point method.

Bridge Name	2nd Humen	Lingding Channel	Shuangyumen	Sunda Strait
μ_{K1}	1	1	1	1
σ_{K1}	0.05	0.05	0.05	0.05
μ_{re}	77.4	84.0	84.1	93
σ_{re}	5.8	6.3	6.3	7.0
μ_{K2}	1.22	1.22	1.22	1.22
σ_{K2}	0.09	0.09	0.09	0.09
μ_{ac}	27.24	36.04	36.10	40.05
σ_{ac}	5.45	7.21	7.22	8.01

Table 17. Mean values and standard deviations of fundamental variables for four proposed bridges.

Bridge Name	Method	β	P_F	T_{ac}
2nd Humen	Central	3.3264	4.40e-04	2273
	Checking	3.3725	3.72e-04	2685
Lingding Channel	Central	2.6494	4.03e-03	248
	Checking	2.6803	3.68e-03	272
Shuang-yumen	Central	2.6481	4.05e-03	247
	Checking	2.6793	3.69e-03	271
Sunda Strait	Central	2.6367	4.19e-03	239
	Checking	2.6668	3.83e-03	261

Table 18. Robustness evaluation of flutter stability for four proposed bridges based on two methods.

Conclusions

Aerodynamic stabilization challenges of long-span cable-supported bridges have been introduced and discussed with seven cable-stayed bridges and eight suspension bridges. The top five completed cable-stayed bridges with spatial cable plane and steel box girder have good enough dynamic and aerodynamic

characteristics, and the high enough critical speeds for aerodynamic flutter and aerostatic divergence may support to longer spans of 1400~1500m with cantilever horizontal stabilization plate or twin box deck. Based on the top three completed suspension bridges, the intrinsic limit of span length due to aerodynamic flutter is about 1,500m for a traditional suspension bridge either with a box or truss girder, and stabilizer, slot and their combination could be prepared if beyond or even approaching this limit. Some new aerodynamic stabilization countermeasures have been developed and proposed, for example, the 2nd Humen Bridge with horizontal stabilizers, Lingding Channel Bridge with vertical and horizontal stabilizer combination, Shuangyumen Bridge and Sunda Strait Bridge with optimization of twin box girder and Taiwan Strait Bridge with widely slotted box girder or narrowly slotted box with stabilizers.

Robustness evaluation for aerodynamic stability have been proposed and discussed for long-span cable-supported bridges. The robustness evaluation method is formulated as a limit state up-crossing model, a probability calculation approach and three evaluation indexes, including reliability index, failure probability and return period. Two approaches based on the first order reliability method have been used in calculating the return period of eight cable-supported bridges, as numerical examples.

Acknowledgement

The work described in this paper is partially supported by the NSFC under the Grants 90215302 and 51323013 and by the MOST under the Grants 2013CB036301 and SLDRCE10-A-01.

References

[1] Gimsing, N.J., *Cable Supported Bridges Concept and Design*, John Wiley & Sons, 1983.

[2] Ge, Y.J., *Wind Resistance of Long Span Suspension Bridges*, People's Communications Press, 2011 (in Chinese).

[3] Ge, Y.J., Xiang, H.F., Aerodynamic challenges in long-span bridges, in *Centenary Conference of the Institution of Structural Engineers*, Hong Kong, China, January 24-26, 2008.

[4] Ge, Y.J., Aerodynamic challenge and limitation in long-span cable-supported bridges, in *2016 World Congress on Advances in Civil, Environmental, and Materials Research (ACEM16)*, Jeju Island, Korea, August 28-September 1, 2016.

[5] Zhu, L.D., Zhang, H.J., Guo, Z.S. and Hu, X.H., Flutter performance and control measures of a 1400m-span cable-stayed bridge scheme with steel box deck, in *13th International Conference on Wind Engineering*, Amsterdam, The Netherlands, July 10-15, 2011.

[6] Zhou, Z.Y., Hu, X.H. and Ge, Y.J., Wind Tunnel Study on Wind Resistance of Qiongzhou Strait Bridge, *Technical Report WT201510*, State Key Laboratory of Disaster Reduction in Civil Engineering at Tongji University (in Chinese).

[7] Internet address 2016, http://en.wikipedia.org.wiki//List_of_longest_suspension_bridges.

[8] Chen, A.R., Guo, Z.S., Zhou, Z.Y., Ma, R.J and Wang, D.L., Study of Aerodynamic Performance of Runyang Bridge, *Technical Report WT200218*, State Key Laboratory of Disaster Reduction in Civil Engineering at Tongji University (in Chinese).

[9] Ge, Y.J., Yang, Y.X., Cao, F.C. and Zhao, L., Study of Aerodynamic Performance and Vibration Control of Xihoumen Bridge, *Technical Report WT200320*, State Key Laboratory of Disaster Reduction in Civil Engineering at Tongji University (in Chinese).

[10] Makoto, K., Technology of the Akashi Kaikyo Bridge, *Structural Control and Health Monitoring*, 2004, 11, 75-90.

[11] Miyata, T., Historical review of long-span bridge aerodynamics, *Journal of Wind Engineering and Industrial Aerodynamics*, 2003, 91, 1393-1410.

[12] Ge, Y.J., Yang, Y.X., Cao, F.C. and Zhao, L., Study of Aerodynamic Performance of the 2nd Humen Bridge, *Technical Report WT201407*, State Key Laboratory of Disaster Reduction in Civil Engineering at Tongji University (in Chinese).

[13] Ge, Y.J., Zhao, L., Cao, F.C and Yang, Y.X., Study of Aerodynamic Performance of Lingding Channel Bridge, *Technical Report WT201505*, State Key Laboratory of Disaster Reduction in Civil Engineering at Tongji University (in Chinese).

[14] Ge, Y.J., Yang, Y.X., Cao, F.C and Zhao, L., Study of Aerodynamic Performance of Shuangyumen Bridge, *Technical Report WT201601*, State Key Laboratory of Disaster Reduction in Civil Engineering at Tongji University (in Chinese).

[15] Zhou, Z.Y., Song, J.Z., Hu, X.H. and Ge, Y.J., Sectional Model Testing of Stiffening Girder of Sunda Strait Bridge, *Technical Report WT201506*, State Key Laboratory of Disaster Reduction in Civil Engineering at Tongji University (in Chinese).

[16] Xiang, H.F. and Ge, Y.J., On aerodynamic limit to suspension bridges, in *11th International Conference on Wind Engineering*, Texas, USA, June 2-5, 2003.

[17] Ge, Y.J. and Xiang, H.F., Tomorrow's challenge in bridge span length, in *IABSE Symposium 2006*, Budapest, Hungary, September 13-15, 2006.

[18] Ge, Y.J. and Xiang, H.F., Great demand and various challenges - Chinese Major Bridges for Improving Traffic Infrastructure Nationwide, in *IABSE Symposium 2007*, Weimar, Germany, September 19-21, 2007.

[19] Knoll F., Vogel T. *Design for Robustness* [M]. Structural Engineering Documents 11, IABSE-AIPC-IVBH, ETH Zurich, 2009.

[20] Ge, Y.J., *Reliability Theory and Application of Wind-induced Vibration of Bridges* [D], Doctoral Dissertation of Tongji University, Supervised by Xiang, H.F., 1997.

[21] Davenport A.G. Comparison of model and full-scale tests on bridges [M]. *Wind Tunnel Modelling for Civil Engineering Applications*, Cambridge University Press, 1982, pp.619-636.

[22] Ministry of Communications, Wind-resistant Design Specification for Highway Bridges (JTG/T D60-01—2004), 2004.

[23] Chen L., Lind N.C. Fast probability integration by three-parameters normal tail approximation, *Structural Safety*, 1983, 1: 269-276.

[24] Benjamin J.R., Cornell C.A., *Probability, Statistics and Decision for Civil Engineers*, McGraw-Hill, Inc., 1970.

[25] Hasofer A.M., Lind N.C., Exact and invariant second moment code format, *Journal of Engineering mechanics Division*, ASCE, 1974, 100: 111-121.